Optics and Laser Technology 116 (2019) 293–299

Contents lists available at ScienceDirect

Optics and Laser Technology

journal homepage: www.elsevier.com/locate/optlastec

Full length article

Temperature tunable Fano resonance based on ring resonator side coupled with a MIM waveguide

Fang Chen*, Huafeng Zhang, Lihui Sun, Jijun Li, Chunchao Yu

Institute of Quantum Optics and Information Photonics, School of Physics and Optoelectronic Engineering, Yangtze University, Jingzhou 434023, People's Republic of China

HIGHLIGHTS

- Fano resonance based on MIM waveguide cavity with a metal nanowall is presented.
- The geometric sizes, temperature effect on Fano resonance is analysis in details.
- The proposed structure may have application in slow light, filter and sensor.

ARTICLE INFO

Keywords:
Surface plasmon polariton
Ring resonator
Fano resonance
Nano sensing

ABSTRACT

The temperature control of Fano resonance via a resonator waveguide system which is composed of a side coupled ring cavity and a metal nanowall is presented. The ring resonator is filled with sealed ethanol which can tune the Fano resonance by the temperature. Two dimensional finite difference time domain method is used to calculate the transmission and field distribution. The Fano resonance is originated from the coupling between the discrete state and the continua state. The discrete state and continua state is from the side coupled ring resonator and the metal nanowall, respectively. The asymmetrical Fano linestyle can be tuned by changing the temperature of the sealed ethanol or the geometric parameters. Multiple Fano resonance can be obtained by introducing another ring resonator and can be tuned by temperature or size independently. The proposed plasmonic structure may have application in slow light device, nanoscale filter, all optical switch and refractive index sensor.

1. Introduction

Surface plasmons (SP) are the light waves that trap on metal-dielectric interface, which has the ability to overcome the classical diffraction limit and regarded as an intriguing field for optical switch, sensing and nano integrating [1–3]. Surface plasmons are considered to have application in the design of precision nanophotonic devices over recent years. Many plasmonic devices based on SPPs have been proposed to realize all optical modulation. Such as wavelength demultiplexers [4], plasmonic sensor [5,6], plasmonic filter [7–9], optical switching [10], slow light [11–13], plasmonic perfect absorber [14,15] have been investigated. Fano resonance exhibits asymmetric and sharp line style which is arises from the constructive and destructive interferences between a sharp discrete state and a broad continuous state. They have been realized in many systems, for example, all dielectric nanoparticle oligomers [16], planar pseudo dolmen structure [17], rod and concentric square ring disk nanostructure [18]. But the metallic nanoparticle structure is not suitable for integration. Recently, Fano resonance is also studied in plasmonic metal-insulator-metal (MIM) waveguide resonator system, The waveguide resonator system has great advantages in refractive index sensing and optical switch due to its sharp and asymmetric line shape. In addition, MIM waveguide is very suitable for integration due to its capability of overcoming the diffraction limit. Single and multiple Fano resonances based on MIM waveguide resonator structure have been designed due to near field coupling. For example, Li et al. investigated Fano resonances based on multimode and degenerate mode interference in plasmonic resonator system [19]. Ouyang et al. proposed and investigated tunable Fano resonance in a MIM waveguide structure coupled with hetero cavities [20]. Meng et al. investigated the control of Fano resonance in photonic crystal nanobeams side coupled with nanobeam cavities and its application in sensing [21]. The coupled mode theory (CMT) is often used to calculate the Fano response, but the cavity mode amplitude and waveguide coupling loss are hard to be analytically obtained. However,

* Corresponding author.
E-mail address: chenfang@yangtzeu.edu.cn (F. Chen).

https://doi.org/10.1016/j.optlastec.2019.03.044
Received 28 November 2018; Received in revised form 25 March 2019; Accepted 26 March 2019

most of the Fano resonances arise from the mode interference in the resonators, which make it hard to tune. Active control of SPPs in plasmonic structure is very valuable because its potential application in the design of tunable plasmonic device. Therefore, there is an urgent need to develop tunable MIM waveguide structure where their optical transmission can be actively tuned by external force, heat, electric, magnetic field and temperature.

Active tunable plasmonic devices can be designed by many optical effects. Such as electro-optic effect, magnetic optic effect, thermo-optic effect, Kerr effect and so on. In our previous paper [22–25], graphene, Kerr material, liquid crystal material and optofluidic technology is utilized in our work to design tunable plasmonic devices. such as all optical switch, plasmonic filter, tunable plasmonic splitter, Fano resonance and sensor. It is worth mentioning that in recent years optofluidic sensing and silicon photonics show great application prospects in biomedical, optical trapping and manipulate nanoscale particles [26–29]. In this work, a Fano resonance structure based on waveguide side coupled ring resonator with metal nanowall is proposed, the ring cavity is filled with sealed ethanol. It is found that the transmittance of the proposed system decreased from peak to dip with wavelength shifts of only 9 nm for the Fano resonance. The Fano resonance tuned by temperature is investigated, the resonant wavelength, peak transmittance, linewidth can also be tuned by the geometric parameters. Moreover, by introducing another ring resonator with different ethanol temperatures or sizes, four Fano resonance can be realized. By controlling the ethanol temperature in the ring resonator, the Fano resonance can be tuned independently. Therefore, the proposed compact plasmonic structure may pave a way for the design of tunable multiple Fano resonance device.

2. Geometry and simulation method

Fig. 1 shows the proposed plasmonic waveguide coupled resonator system which is composed of a MIM waveguide with metal nanowall and a ring resonator. In the simulation, a two dimensional model is used. The metal in the model is silver, and the frequency dependent complex relative permittivity of silver is characterized by the Drude model:

$$\varepsilon(\omega) = 3.7 - \frac{\omega_p^2}{(\omega^2 + i\omega\gamma_p)} \quad (1)$$

Where the plasma frequency of silver is $\omega_p = 1.37 \times 10^{16} s^{-1}$, and the damping constant is $\gamma_p = 2.73 \times 10^{13} s^{-1}$ [30]. The insulator in the MIM waveguide is air. The width of the bus waveguide is w, the thickness of the metal nanowall is s. The outer radius and inner radius of the ring cavity are R and r. The gap between the MIM waveguide and the ring cavity is g. The ring cavity is filled with ethanol, whose refractive index $n = 1.36084 - 3.94 \times 10^{-4}(T - T_0)$, T_0 stands for the room temperature as 20 °C [31]. FDTD solution 8.15 and matlab 7.0 were used for numerically calculated. Since the light is incident from X directions, perfect matched layers (PMLs) are applied in X direction. Metal boundary condition was selected in Y direction. The grid sizes in X and Y are set to be 5 $nm \times 5$ nm , $\Delta t = \frac{\Delta x}{2c}$, where c is the free space speed of light. The total simulation area is 1600 $nm \times 1600$ nm. In this paper, the performance of the proposed Fano resonance has been simulated by 2D FDTD method, assuming the thickness of the z direction is infinite, for actual 3D structure in laboratory, this assumption is acceptable for the thickness larger than 1 um [32]. More accurate results can be obtained by 3D FDTD method but at the cost of a larger number of computer memory and time.

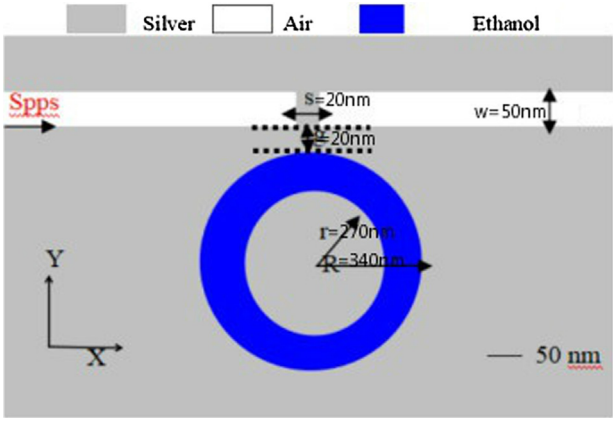

Fig. 1. The schematic diagram of the proposed plasmonic resonator system composed of a ring resonator filled with sealed ethanol and a MIM waveguide separated by a air slot. The geometrical parameters of the proposed plasmonic Fano structure were set as $w = 50$ nm, $s = 20$ nm, $R = 320$ nm, $r = 270$ nm, $g = 20$ nm.

3. Simulation results

In the simulation, the geometric parameters of the proposed structure are set as: $w = 50$ nm, $s = 20$ nm, $R = 320$ nm, $r = 270$ nm, $g = 20$ nm. In the whole paper, the normalized transmittance of the structure is defined as the quotient between the power flows (obtained by integrating the Poynting vector over cross section of the MIM waveguide) of the output and input port. The transmission spectra of the MIM waveguide with metal nanowall, single ring cavity and the whole Fano coupled system are presented in Fig. 2. For the MIM waveguide with a metal nanowall, the transmittance is less than 0.16 in the range of 800–1400 nm. Therefore the metal nanowall can be seen as a continuum state. To creat a discrete state, a ring cavity is side coupled with the MIM waveguide, it can be seen that in the range of 800–1400 nm, there are two symmetric Lorentzian like valleys which represent the first and the second eigenmode of the ring cavity. The two resonance modes are classified by TM_m. m is the number of nodes of standing waves in the ring cavity. From Fig. 3 it can see that the resonant modes are TM_6 and TM_8, respectively. Since the two narrow resonant modes are overlapped with the broad continuum state. Therefore, two sharp and asymmetric Fano resonances are formed in the transmission spectrum. Here, the two Fano resonance are denoted as FR 1 (right Fano resonance in Fig. 2) and FR 2 (left Fano resonance in Fig. 2). The transmittance is about 36% at the peak wavelength 904 nm, and the transmittance is almost zero at 913 nm. The changes of wavelength from peak to dip are 9 nm (FR2), 14 nm (FR1), respectively. Comparing

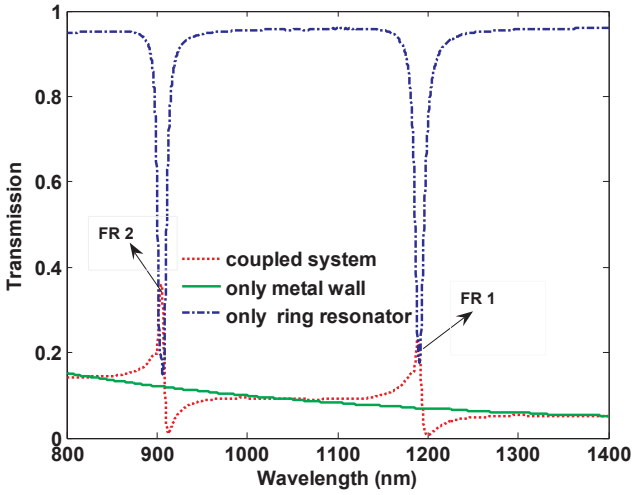

Fig. 2. The FDTD simulation results. The transmission spectra of the single metal nano wall, single ring resonator, and coupled waveguide plasmonic structure.

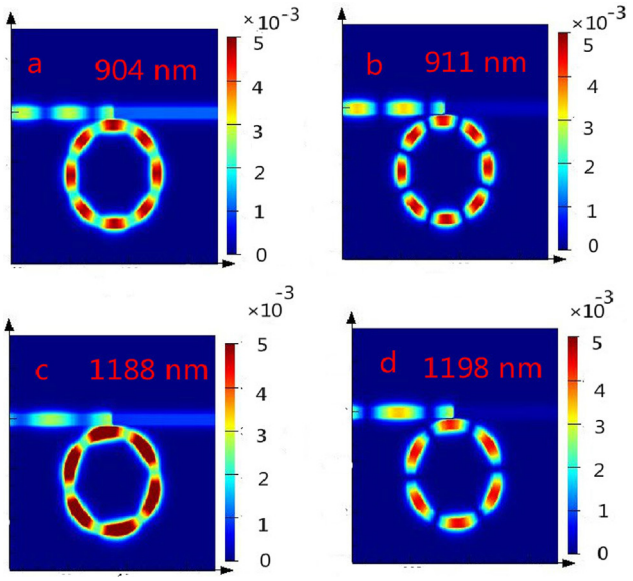

Fig. 3. Magnetic field distributions ($|H_z|$) at the wavelength 904 nm (a), 911 nm (b), 1188 nm (c), 1198 nm (d), respectively.

with the paper, the FR1 in our work is much smaller [33]. Therefore, the sharp Fano resonance (Fig. 2) can be used to design slow light and refractive index sensors.

To further understand the physical mechanism of the Fano resonance, the magnetic field distributions $|H_z|$ at the wavelength of the two transmission peaks (904 nm, 1188 nm) and two transmission dips (911 nm, 1198 nm) are demonstrated in Fig. 3. For comparison, all the field distribution Figs are normalized, and the color bar values are identical. It can be observed from Fig. 3a and c that the a part of SPPs can pass through the bus waveguide. Strong field is confined in the ring cavity. The profile of $|H_z|$ for the plasmonic system at the dip wavelength are displayed in Fig. 3b and d. It can see that the field in the ring resonator and the waveguide causes destructive interference and most of the input energy cannot pass through the bus waveguide. The ultra-narrow Fano spectral line indicates that high on-off contrast ratio can be achieved and has potential application in ultrafast optical switches or filters.

The Fano resonance can be tuned by the geometrical parameters of the ring resonator or the metal nanowall. The effect of gap $g$on the transmission spectra is studied. Here, the other geometric parameters are the same as above in the simulation calculation, when gap $g = 20\ ,\ 25\ ,\ 30\ nm$, the transmission spectrum is displayed in Fig. 4. It can see that when the gap g increases, the transmittance becomes smaller, and at the same time the linewidth becomes also smaller. In particular we found when $g \geqslant 70$ nm, the Fano resonance disappeared since the coupled strength is so small. Therefore, the high contrast ratio and narrow linewidth can be tuned by changing the gap g. As the discrete states is induced by the ring resonator. The effect of the radius of ring resonator on the transmission spectra is investigated and the results validating it can affect the spectral. Keep the other parameters the same as above, from Fig. 5 it can be observed that the Fano peak wavelength red shift when the outer radius of the ring resonator increases from 320 nm to 325, 330, 335, and 340 nm. This is because in the proposed Fano resonance, the two discrete states are provided by the side coupled ring resonator, the position of two Fano peaks is directly affected by the positions of the two resonant modes of the ring resonator.

In the proposed Fano resonance, the continua state is induced by the metal nanowall, the effect of the thickness of the metal nanowall on the transmission spectra is calculated. From Fig. 6, it can be seen that when the thickness of the metal nanowall increase, the transmittance of the

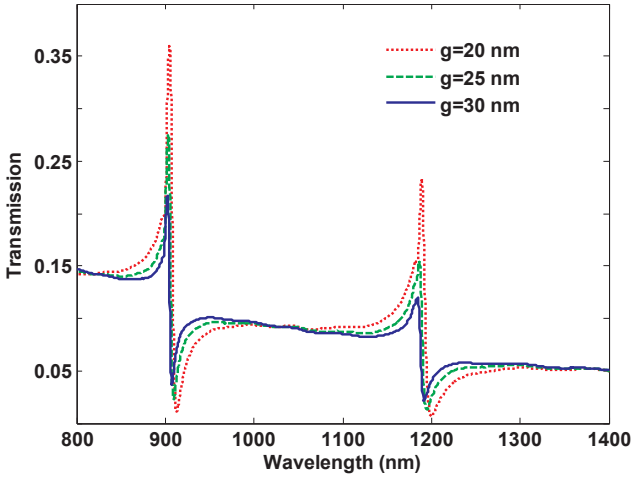

Fig. 4. The transmission spectra of the plasmonic Fano system with different gap distances g.

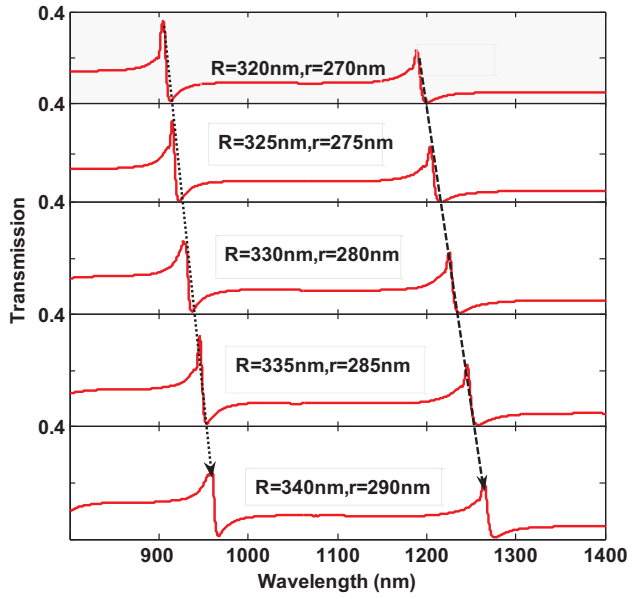

Fig. 5. The transmission spectra of the plasmonic Fano system with different ring cavity radius R.

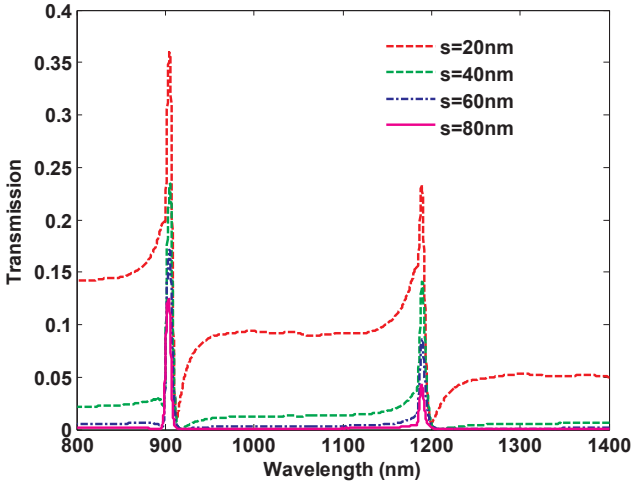

Fig. 6. The transmission spectra of the plasmonic Fano system with different thickness of metal nanowall s.

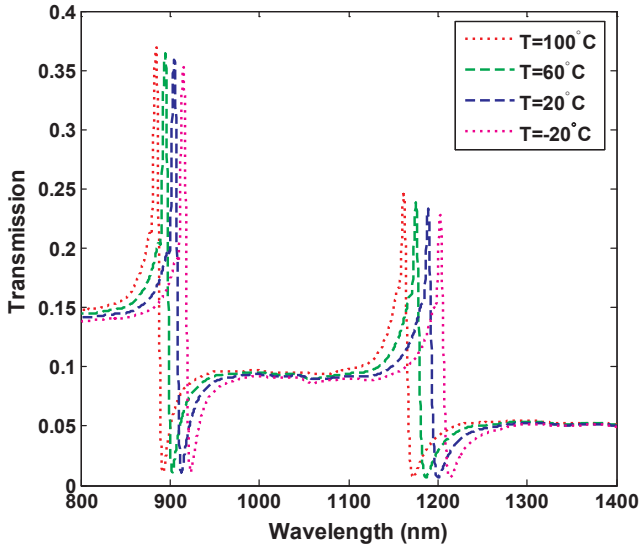

a

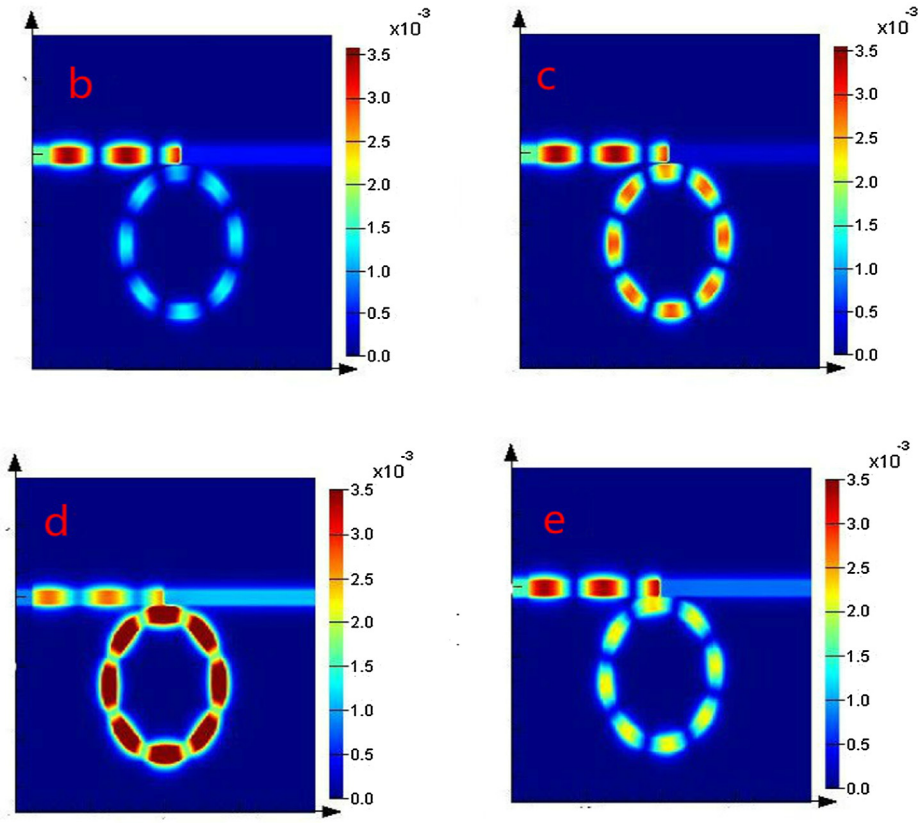

Fig. 7. (a) The transmission spectra of the plasmonic Fano system with different temperatures to ethanol filled in the ring cavity. FDTD simulations of the time averaged magnetic field ($|H_z|$) ($\lambda = 905nm$) intensity distribution when (b) $T = 100$ ˚C (c) $T = 60$ ˚C (d) $T = 20$ ˚C (e) $T = -20$ ˚C.

Fano resonance becomes smaller, and the Fano resonance effect becomes weaker, especially when the thickness of the metal nanowall increases to 80 nm, the continua state is almost disappeared, and the transmission spectrum takes on a symmetric Lorentzian linestyle. The above characteristics indicate that we can tune the Fano resonance by changing the thickness of the metal nanowall.

The refractive index of the ethanol can be tuned by the temperature, therefore the Fano resonance peaks can be tuned by the temperature. Fig. 7(a) shows the transmission spectra of the plasmonic Fano system with different temperatures to the ring cavity. According to our simulations, as the temperature of the ethanol increases, the Fano resonance wavelength is blue shifted. A 41 nm change of FR 1 has been achieved by increasing the temperature from $T = -20$ ˚C to $T = 100$ ˚C, the corresponding frequency shift is about $\Delta f = 258.1THz - 249.3THz = 8.8THz$. FDTD simulations of the time averaged magnetic field (905 nm) intensity distributions are presented in Fig. 7(b)–(e). Taking the Fig. 7d as an example, it is the field distributions at the resonant wavelength (transmission peak 905 nm) of the left Fano resonance. It can be see a standing wave pattern with strong field intensities is excited in the ring resonator. There are eight

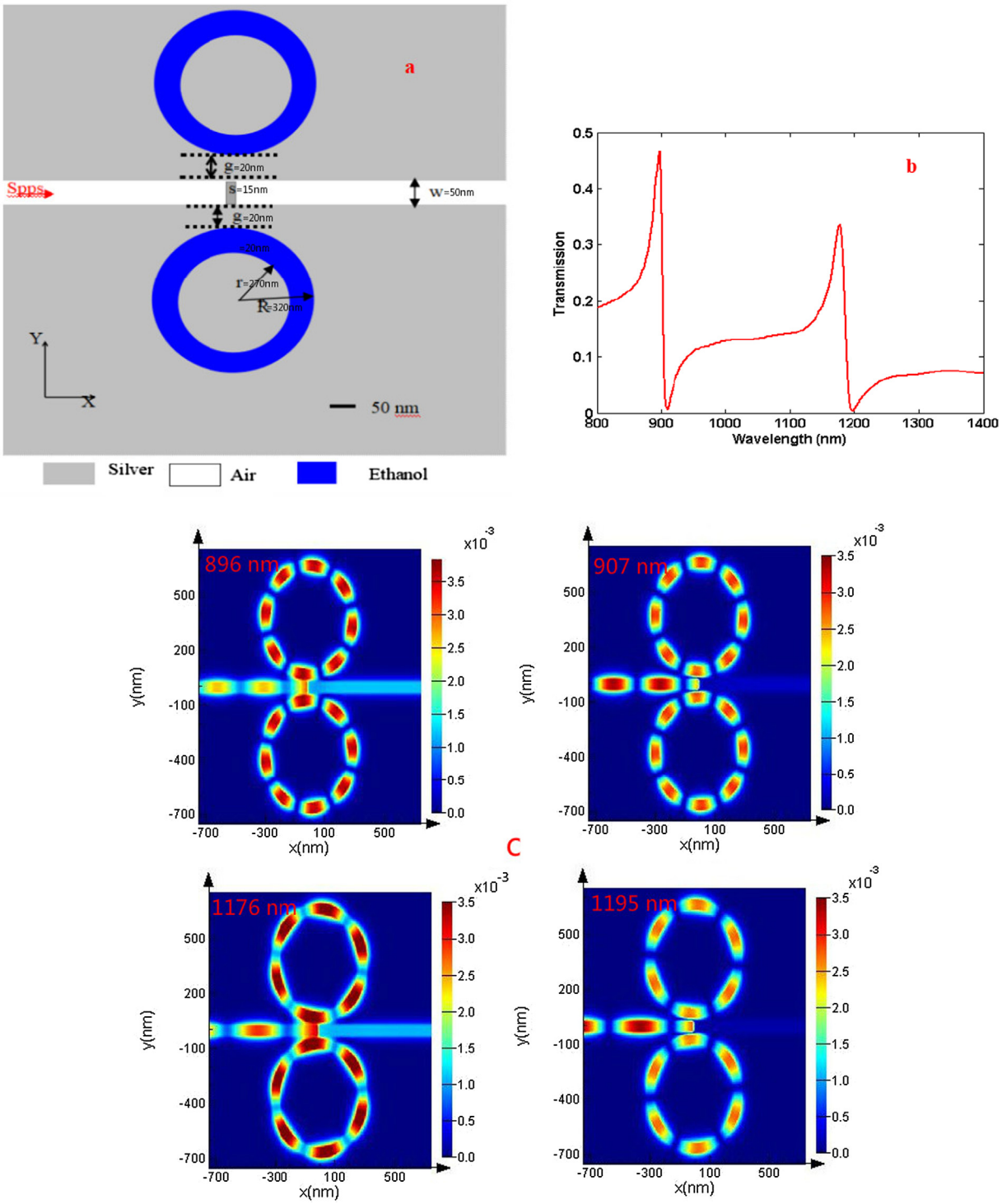

Fig. 8. a. The schematic of the plasmonic Fano system consisting of two side coupled ring resonators and a metal nanowall. b. The transmission spectrum of the two same ring resonators side coupled Fano system ($T_1 = T_2$). c. shows the corresponding Magnetic field distributions ($|H_z|$) at the peaks and dips wavelength. The other geometrical parameters of the proposed plasmonic Fano structure were set as $w = 50\ nm$, $R = 320\ nm$, $r = 270\ nm$, $g = 20\ nm$, $s = 15\ nm$.

anti-nodes in the standing wave pattern, revealing that a high order resonant mode (eight order oscillation) is excited in the ring resonator. For the eight order oscillation, at the connection part between the MIM waveguide and the ring resonator is a node, as shown in Fig. 7d. It makes the power flow of the node in the ring resonator difficult to be leaked in to the MIM waveguide, and thus the power of the eight order mode is trapped in the ring resonator. Therefore, the eight order resonant mode is a strong trapped mode with a narrow response spectrum (FR 1). By increasing the temperature, the refractive index n of the ethanol decrease, the optical length of the ring resonator ($s = 2\pi r_{eff}\mathrm{Re}(n_{eff})$) decrease as well, where n_{eff} refers to the effective refractive index of the ring resonator, which can be solved by the dispersion equation, r_{eff} is the effective radius of the ring resonator. The resoannce condition of the cavity mode is $m\lambda = s$, $m = 1, 2\ldots$ There, the resonant frequency and the quantity of transmitted light will be varied with the temperature. Therefore, the proposed plasmonic waveguide structure can be

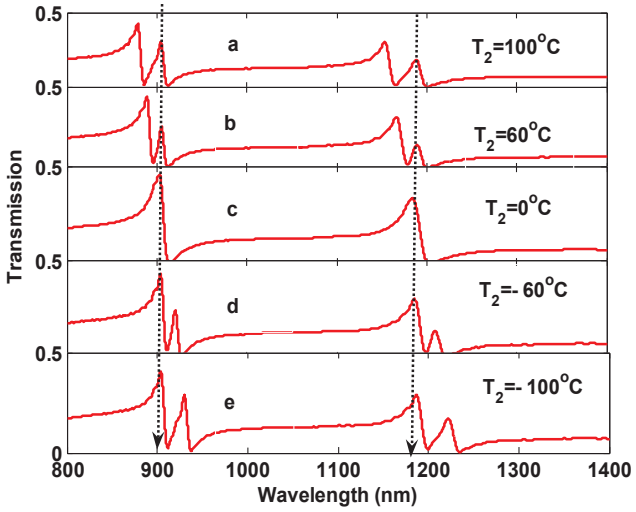

Fig. 9. The transmission spectrum of the side coupled two ring resonators with different temperatures T_2 of ethanol in the lower resonator, and the temperature of ethanol in upper resonator are fixed at $T_1 = 0$ ˚C.

used as a tunable Fano resonance devices.

One way to realize multiple Fano resonance is to introduce another side coupled ring resonator in the above structure. For symmetry structure, as can be seen from Fig. 8a, the two ring resonators have the same size. When the ethanol temperature in the two ring resonators are the same ($T_1 = T_2$), the transmission spectrum is shown in Fig. 8b, it can be seen that two Fano resonances appear in the transmission spectrum. The Magnetic field distributions ($|H_z|$) at the peaks and dips wavelength are shown in Fig. 8c. The field distributions are symmetry due to the proposed symmetrical structure. However, by introducing asymmetry, when the ethanol temperature in the two ring resonators are not the same ($T_1 \neq T_2$), the ethanol temperature in the upper resonator is set $T_1 = 0^0C$and keep unchanged, but the ethanol temperature in the lower resonator T_2 changes from 100 ˚C to 60 ˚C, 0 ˚C, −60 ˚C and −100 ˚C. The transmission spectra are shown in Fig. 9, it can be seen that there are four Fano resonances in the spectra. In order to investigate the physical mechanism of the four Fano resonance, the Magnetic field distributions ($|H_z|$) at the peaks and dips wavelength are shown in Fig. 10 when $T_2 = -100$ ˚C. Obviously, it can be seen that the field energy is confined in the upper resonator when the wavelength are 930 nm, 938 nm, 1222 nm and 1236 nm. While the field energy is confined in the lower resonator when the wavelength are 904 nm, 912 nm, 1187 nm and 1200 nm. When the ethanol temperature in the lower resonator T_2 decreases, the Fano resonances (904 nm and 1187 nm) keep unchange, but the other two Fano resoannces (930 nm and 1222 nm) show an obvious red shift behavior. This phenomenon indicates that the Fano resonances (904 nm and 1187 nm) are related to lower resonator and the Fano resoannces (930 nm and 1222 nm) are related to upper resonator. Moreover, the sensitivity of the proposed temperature sensor is calculated and the results is 0.31 nm/˚C, which is bigger than the value reported in the paper [34,35]. Another way to introduce asymmetry is to change the size of the lower ring resonator, we set the size of upper resonator $R = 320\ nm$, $r = 270\ nm$ and keep unchanged, but the size of the lower resonator changes from $R = 325\ nm$, $r = 275\ nm$ to $R = 330\ nm$, $r = 280\ nm$, $R = 335\ nm$, $r = 285\ nm$, $R = 340\ nm$, $r = 290\ nm$ and $R = 345\ nm$, $r = 295\ nm$. The evolution of quadruple Fano resonances are shown in Fig. 11. The above quadruple Fano resonance can be tuned independently by using different temperatures in the two resonators or ring size. Due to the physics origin as an interference phenomenon and the sharp asymmetric line shape, the devices based on Fano resonance have shown a large sensitivity and figure of merit (FOM), which can be used in sensors, switch and slow light. Since spectral transmittance

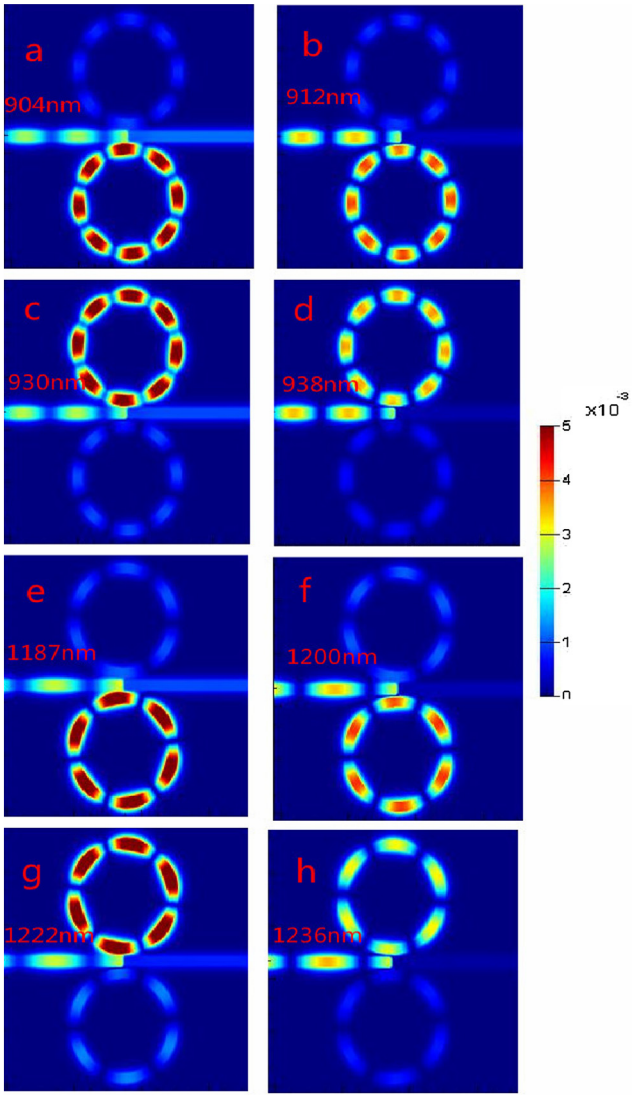

Fig. 10. Magnetic field distributions ($|H_z|$) of the plasmonic system when $T_1 = 0$ ˚C and $T_2 = -100$ ˚C at the Fano resonance dips and peaks.

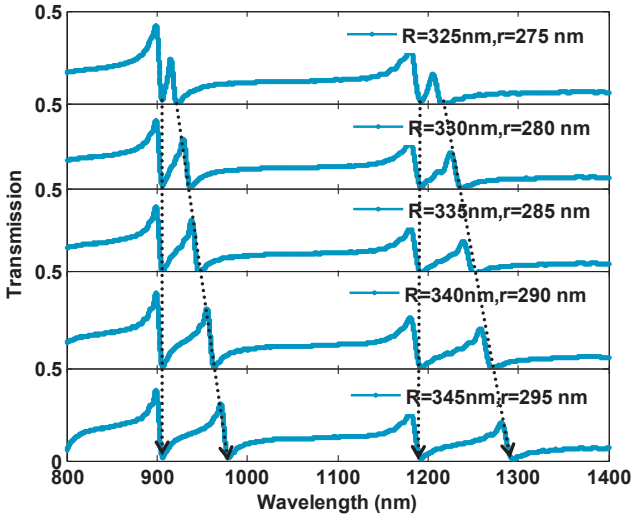

Fig. 11. The transmission spectrum of the side coupled two ring resonators with different sizes of the lower resonator, and the size of upper resonator is fixed at $R = 320\ nm$, $r = 270\ nm$.

drops sharply from peak to dip, the asymmetric spectral shape induced by Fano resonance is capable of retrieving high sensitive temperature measurements, the sensitivity of the proposed temperature sensor is 0.31 $nm/^{\circ}C$, which is bigger than the paper [34,35].

4. Conclusions

In this paper, the Fano sharp line shape has been investigated numerically in plasmonic waveguide systems which consist of a metal nanowall and ring cavity. Ethanol in the ring cavity which can been used to modulate the Fano resonance. Numerical calculation results indicate that the Fano resonant wavelength, transmittance and line width can be tuned by the geometric parameters. Such as the thickness of the metal nanowall, the radius of the ring cavity, the gap between the MIM waveguide and ring cavity. Moreover, the Fano resonance can also be tuned by the temperature of the ethanol. Multiple Fano resonance can be tuned by controlling the temperature of ethanol or the ring size. The above results can find potential applications in highly integrated circuits, optical switch, plasmonic nanosensor and slow light devices.

Acknowledgments

Funding: Supported by The Yangtze Youth Fund (Grant No. 2016cqn55), Yangtze Fund for Youth Teams of Science and Technology Innovation (Grant No. 2015cqt03). National Natural Science Foundation of China (Grant No. 11747091).

Appendix A. Supplementary material

Supplementary data to this article can be found online at https://doi.org/10.1016/j.optlastec.2019.03.044.

References

[1] K.F. MacDonald, Z.L. Samson, M.I. Stockman, N.I. Zheludev, Ultrafast active plasmonics, Nat. Photon. 3 (2009) 55–58.
[2] W.L. Barnes, A. Dereux, T.W. Ebbesen, Surface plasmon subwavelength optics, Nature 424 (2003) 824–830.
[3] N. Liu, T. Wesis, M. Mesch, L. Langguth, U. Eigenthaler, M. Hirscher, C. Sonnichsen, H. Giessen, Planar metamaterial analogue of electromagnetically induced transparency for plasmonic sensing, Nano Lett. 10 (2010) 1103–1107.
[4] Z. Chen, R. Hu, L.N. Cui, L. Yu, L.L. Wang, J.H. Xiao, Plasmonic wavelength demultiplexer based on tunable Fano resonance in coupled-resonator systems, Opt. Commun. 320 (2014) 6–11.
[5] Hua Lu, Xueming Liu, Dong Mao, Guoxi Wang, Plasmonic nanosensor based on Fano resonance in waveguide-coupled resonators, Opt. Lett. 37 (18) (2012) 3780.
[6] F. Hao, Y. Sonnefraud, D.P. Van, S.A. Maier, N.J. Halas, P. Nordlander, Symmetry breaking in plasmonic nanocavities: subradiant LSPR sensing and a tunable Fano resonance, Nano Lett. 8 (3983) (2008) 3988.
[7] H. Lu, X.M. Liu, Y.K. Gong, L.R. Wang, D. Mao, Multi-channel plasmonic waveguide filters with disk-shaped nanocavities, Opt. Commun. 284 (2011) 2613–3266.
[8] T. Xu, Y.K. Wu, X.G. Luo, L.J. Guo, Plasmonic nanoresonators for high-resolution colour filtering and spectral imaging, Nat. Commun. 1 (2010) 59.
[9] X.S. Lin, X.G. Huang, Tooth-shaped plasmonic waveguide filters with nanometeric sizes, Opt. Lett. 33 (23) (2008) 2874–2876.
[10] D.M. Beggs, T.P. White, L.O. Faolain, T.F. Krauss, Ultracompact and low-power optical switch based on silicon photonic crystal, Opt. Lett. 33 (2008) 147–149.
[11] C. Wu, A.B. Khanikaev, G. Shvets, Broadband slow light metamaterial based on a double-continuum Fano resonance, Phys. Rev. Lett. 106 (10) (2011) 10742.
[12] K. Totsuka, N. Kobayashi, M. Tomita, Slow light in coupled-resonator-induced transparency, Phys. Rev. Lett. 98 (21) (2007) 213904.
[13] G. Lai, R.S. Liang, Y.J. Zhang, Z.Y. Bian, L.X. Yi, G.Z.M. Zhan, R.T. Zhao, Double plasmonic nanodisks design for electromagnetically induced transparency and slow light, Opt. Exp. 23 (5) (2015) 6554–6561.
[14] Y. Bai, L. Zhao, D.Q. Ju, Y.Y. Jiang, L.H. Liu, Wide angle, polarization independent and dual band infrared perfect absorber based on L-shaped metamaterial, Opt. Exp. 23 (5) (2015) 8670–8680.
[15] B.X. Zhang, Y.H. Zhao, Q.Z. Hao, B. Kiraly, I.C. Khoo, S.F. Chen, T.J. Huang, Polarization independent dual band infrared perfect absorber based on a metal dielectric metal elliptical nanodisk array, Opt. Exp. 19 (16) (2011) 15222–15228.
[16] K.E. Chong, B. Hopkins, I. Staude, A.E. Miroshnichenko, J. Dominguez, M. Decker, D.N. Neshev, I. Brener, Y.S. Kivshar, Observation of Fano resonances in all dielectric nanoparticle oligomers, Small (2014) 1985–1990.
[17] N. Li, X.J. Tian, W. Zhang, L.N. Luo, G. Li, Z.Y. Zhang, Double Fano resonances in a planar pseodu-dolmen structure, Sensor Actuat. A: Phys. 234 (2015) 346–350.
[18] Y.Y. Huo, T.Q. Jia, Y.Z. Zhang, H. Zhao, S.A. Zhang, D.H. Feng, Z.R. Sun, Narrow and deep fano resonances in a rod and concentric square ring disk nanostructures, Sensors 13 (11350) (2013) 11361.
[19] S.L. Li, Y.L. Wang, R.Z. Jiao, L.L. Wang, G.Y. Duan, L. Yu, Fano resonances based on multimode and degenerate mode interference in plasmonic, Opt. Exp. 25 (2017) 3525–3533.
[20] Q. Wang, Z.B. Ouyang, M. Lin, Q. Liu, Independently tunable Fano resonance based on the coupled hetero cavities in a plasmonic MIM system, Materials 11 (2018) 1675.
[21] Z.M. Meng, Z.Y. Li, Control of Fano resonance in photonic crystal nanobeams side coupled with nanobeam cavities and their applications to refractive index sensing, J. Phys. D Appl. Phys. Accept (2018).
[22] F. Chen, A tunable high-efficiency optical switch based on graphene coupled photonic crystal structure, J. Mod. Opt. 64 (2017) 1531–1537.
[23] F. Chen, D.Z. Yao, Y.N. Liu, Graphene-metal hybrid plasmonic switch, Appl. Phys. Exp. 7 (2014) 082202.
[24] F. Chen, D.Z. Yao, Optofluidic tunable plasmonic filter based on liquid-crystal microcavity structure, J. Mod. Opt. 61 (2014) 1486–1491.
[25] F. Chen, D.Z. Yao, Tunable multiple all-optical switch based on multi-nanoresonator coupled waveguide systems containing Kerr material, Opt. Commun. 312 (2013) 143–147.
[26] Y.Z. Shi, S. Xiong, L.K. Chin, Y. Yang, J.B. Zhang, W. Ser, J.H. Wu, T.N. Chen, Z.C. Yang, Y.L. Hao, B. Liedberg, P.H. Yap, Y. Zhang, A.Q. Liu, High-resolution and multi-range particle separation by microscopic vibration in an optofluidic chip, Lab. Chip 17 (2017) 2443–2450.
[27] Y.Z. Shi, S. Xiong, Y. Zhang, L.K. Chin, Y.Y. Chen, J.B. Zhang, T.H. Zhang, W. Ser, A. Larson, L.S. Hoi, J.H. Wu, T.N. Chen, Z.C. Yang, Y.L. Hao, B. LiedbeRg, P.H. Yap, D.P. Tsai, C.W. Qiu, A.Q. Liu, Sculpting nanoparticle dynamics for single-bacteria-level screening and direct binding-efficiency measurement, Nat. Commun. 9 (2018) 815.
[28] Y.Z. Shi, S. Xiong, L.K. Chin, J.B. Zhang, W. Ser, J.H. Wu, T.N. Chen, Z.C. Yang, Y.L. Hao, B. Liedberg, P.H. Yap, D.P. Tsai, C.W. Qiu, A.Q. Liu, Nanometer-precision linear sorting with synchronized optofluidic dual barriers, Sci. Adv. 4 (2018) eaao0773.
[29] M. Ren, J.G. Huang, H. Cai, J.M. Tsai, J.X. Zhou, Z.S. Liu, Z.G. Suo, A.Q. Liu, Nano optomechanical actuator and pull-back instability, Acs Nano 7 (2018) 1676–1681.
[30] H. Lu, X.M. Liu, D. Mao, Y.K. Gong, G.X. Wang, Induced transparency in nanoscale plasmonic resonator systems, Opt. Lett. 36 (3233) (2011) 3235.
[31] T.S. Wu, Y.M. Liu, Z.Y. Yu, H. Ye, Y.W. Peng, C.G. Shu, S.H. Yang, W. Zhang, H.F. He, A nanometeric temperature sensor based on plasmonic waveguide with an ethanol-sealed rectangular cavity, Opt. Commun. 339 (2015) 1–6.
[32] Z. He, H. Li, B. Li, Z. Chen, H. Xu, M. Zheng, Theoretical analysis of ultrahigh figure of merit sensing in plasmonic waveguides with a multimode stub, Optic Lett. 41 (2016) 5206.
[33] J.H. Yang, X.K. Song, Z. Chen, L.N. Cui, S. Yang, L. Yu, Tunable multi Fano resonances in MDM- based side-coupled resonator system and its application in nanosensor, Plasmonics 12 (2017) 1665–1672.
[34] J. Fan, J. Zhang, P. Lu, M. Tian, J. Xu, D. Liu, A single mode filter sensor based on core-offset inter-modal interferometer, Opt. Commun. 320 (2014) 33–37.
[35] T. Srivastave, R. Das, R. Jha, Highly sensitive plasmonic temperature sensor based on photonic crystal surface plasmon waveguide, Plasmonics 8 (2013) 515–521.